

hERG Function in Light of Structure

Gail A. Robertson^{1,*} and João H. Morais-Cabral^{2,3}

¹Department of Neuroscience, School of Medicine and Public Health, University of Wisconsin-Madison, Madison, Wisconsin; ²i3S, Instituto de Investigação e Inovação em Saúde and ³IBMC- Instituto de Biologia Molecular e Celular, Universidade do Porto, Porto, Portugal

ABSTRACT The human ether-a-go-go-related gene1 (hERG) ion channel has been the subject of fascination since it was identified as a target of long QT syndrome more than 20 years ago. In this Biophysical Perspective, we look at what makes hERG intriguing and vexingly unique. By probing recent high-resolution structures in the context of functional and biochemical data, we attempt to summarize new insights into hERG-specific function and articulate important unanswered questions. X-ray crystallography and cryo-electron microscopy have revealed features not previously on the radar—the “nonswapped” transmembrane architecture, an “intrinsic ligand,” and hydrophobic pockets off a pore cavity that is surprisingly small. Advances in our understanding of drug block and inactivation mechanisms are noted, but a full picture will require more investigation.

Structure-function studies of ion channels are problematic. Functional studies provide insights into dynamic transitions between different conformational states but allow only inferences of structure. These approaches require a certain cleverness in design and necessarily involve a simple molecular interpretation. Structural approaches, on the other hand, enable a satisfying visualization of many structural details of the channel, often at the atomic level. But the picture is a static one and of a protein that is sometimes modified by deleting parts of the channel or attaching antibodies to increase stability and monodispersity required for structural and biochemical studies. Only after iterative advances in both regards can we hope to deeply understand our favorite ion channels.

A different intersubunit architecture

More than two decades of combined functional and structural efforts have shed light on the fascinating family of KCNH channels and its most charismatic member, the human ether-a-go-go-related gene1 channel (hERG, encoded by *KCNH2*). Recent single-particle cryo-electron microscopy (cryo-EM) structures of the hERG channel (1) and the rat ether-a-go-go1 channel complexed with four CaM/Ca²⁺ molecules (rEAG, encoded by *KCNH1*) (2) punctuate these advances with new insights. For example, a novel molecular architecture dictates differences with respect to other

voltage-gated K channels for the mechanism of how changes in membrane voltage gate the channel open and closed. Although possessing a canonical S1-S4 voltage sensor domain (VSD), the means by which the VSD connects to the S6 gate is different from other Kv channels. The VSD in KCNH channels is closely apposed to the pore module in the same subunit, the two connected by a short linker (Fig. 1). In contrast, in other Kv channels, the VSD of one subunit interacts with the pore domain of the adjacent subunit. The VSD connects with its own pore domain through a long S4-S5 helical linker, and four S4-S5 linkers form a cuff around the S6 gate sequences. These differences explain why integrity of the S4-S5 linker is required for coupling between the VSD and pore gate in *Shaker*-like channels (3) but not KCNH channels (4,5). In this regard, KCNH channels echo their ligand-gated cousins, the cyclic nucleotide-gated and modulated channels, which also exhibit a “nonswapped” subunit architecture (6,7). Changes in membrane potential must be transduced directly from transmembrane interactions of VSD and pore domains, as has been demonstrated for the HCN1 channel (8) as well as EAG-HCN1 chimeras (9).

An open and a closed channel

The hERG cryo-EM structures show a channel with the VSD in the activated state and the gate open (1). The rEAG structure provides a view of a different conformational state, with the gate closed (2) (Fig. 2 a). This is visible by superimposing the pores of the two channels, showing how S6 of hERG, relative to rEAG, has swung away from the pore axis, creating an entry to the pore cavity large

Submitted August 13, 2019, and accepted for publication October 2, 2019.

*Correspondence: garobert@wisc.edu

Editor: Vasanthi Jayaraman.

<https://doi.org/10.1016/j.bpj.2019.10.010>

© 2019 Biophysical Society.

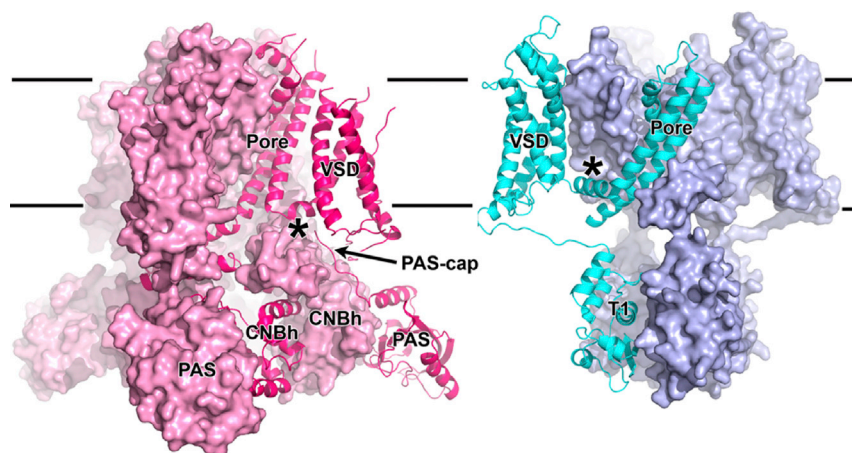


FIGURE 1 hERG and Kv channel. View of the hERG channel (*left*, in *pink*) and Kv1.2-Kv2.1 chimera (*right*, in *cyan*) channels with three subunits shown as surface and the fourth subunit as cartoon. The VSD from a subunit of the Kv chimera was omitted to facilitate view of the pore domain. Star symbols (*) indicate the S4-S5 linkers, which are much shorter in hERG. Lines mark membrane limits. Domains are labeled.

enough to accommodate ion flux (Fig. 2 *b*). S5 follows a parallel change. When the cytosolic gate opens, akin to the blades of a camera iris, a corresponding movement occurs in the two first helices of the C-linker ($\alpha A'$ and $\alpha B'$; Fig. 2 *c*).

It is important to note that both hERG and rEAG channel structures show the S4 voltage sensor in the up position, which agrees well with the electrical field of 0 mV in the experimental setup and the open gate of the hERG channel but not with the conformational state of the closed rEAG. Like other members of the EAG subfamily, rEAG is inhibited by calmodulin in complex with Ca^{2+} (CaM/ Ca^{2+}) (10–14), and the structure provides an extraordinary view of the two proteins together. CaM/ Ca^{2+} either stabilizes the closed gate, forces it closed, or somehow decouples it from the VSDs while they remain in their “up” or activated positions. Thus, we do not yet have a picture of the resting VSD in concert with the closed gate. An interaction between the C-terminus of S4 and the C-linker, covalently

attached to the gate, are proposed to mediate channel closure (2).

Per-Arnt-Sim and cyclic nucleotide-binding domain interactions in the context of the channel

Unique to the KCNH family is its cytosolic complex of the N-terminal region with homology to Per-Arnt-Sim (PAS) domains (15,16) and the C-terminal region with homology to cyclic nucleotide-binding (CNBh) domains (Fig. 1; (17–19)). The cryo-EM structures of hERG and rEAG reveal a cytosolic ring structure with the PAS domain of one subunit interacting with the CNBh domain of its neighbor (Fig. 1; (1,2)). It is unsurprising that the versatile PAS domain, which mediates functions across the phylogenetic spectrum as diverse as phototransduction and redox sensing (20–22), should have evolved a role in gating. Not to be outdone, the C-terminal binding partner has evolved from ancient CNBh domains but is indifferent to cyclic

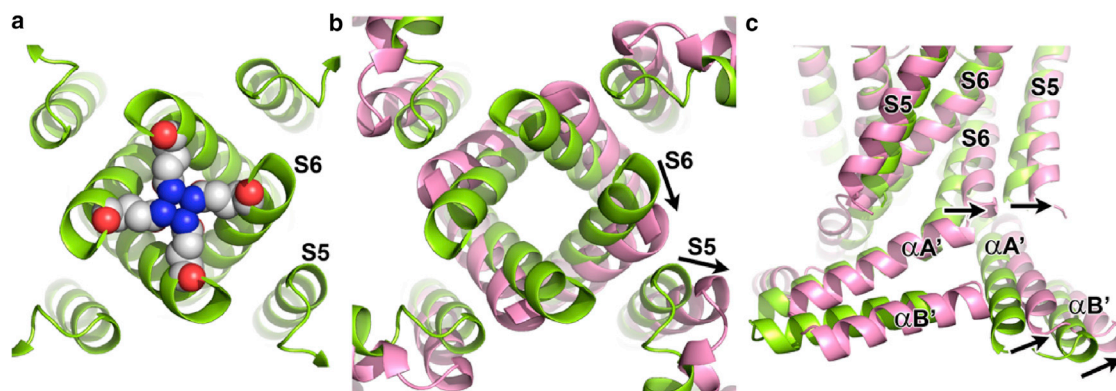


FIGURE 2 Cytosolic gate. (*a*) A view of rEAG channel gate from the cytosol. Residues occluding access to the pore (Q476) are shown as spheres. (*b*) Superposition of hERG (*pink*) and rEAG (*light green*) channels without gate side chains viewed as in (*a*). Displacement of S6 and S5 helices during gating is suggested by arrows in one subunit. (*c*) The gate region of superposed hERG and rEAG viewed from the membrane. Displaced S6 and S5 helices around the gate region of the pore domain are indicated. The N-terminal helices of the C-linker are also visible, showing similar displacement of hERG relative to rEAG.

nucleotides (23,24). Instead, as revealed in the x-ray crystal structures of purified domains, the binding pocket is occupied by a downstream sequence of three amino acids that have assumed the role of “intrinsic ligand” (18,25). KCNH channels are neither modulated nor bound by cyclic nucleotides (23,24); this is not because the intrinsic ligand prevents cyclic nucleotide molecules from binding, but because the side-chain chemistry within the binding pocket has coevolved to interact with the intrinsic ligand (18,25). The ligand lies at the PAS-CNBh domain interface known to be critical for channel function as a hotspot for disease mutations mediating type 2 long QT syndrome (hERG) and cancer (EAG1) (19). Interactions between PAS and CNBh domains appear to be somewhat dynamic, showing, e.g., rearrangements revealed by transition-metal Förster resonance energy transfer (FRET) during gating in ELK (26), another KCNH family member, or alterations in hERG deactivation gating mediated by PAS-directed single-chain variable antibodies (27).

It is interesting to note that mutations in the intrinsic ligand have a range of phenotypes in different KCNH channel types but ultimately suggest a unifying mechanism by which the intrinsically liganded gating ring promotes activation. In hERG channels, the two liganding side chains (in the sequence F860-N861-L862) exert an additive effect stabilizing the open state as measured by combined FRET and gating assays (28). The same is true for human EAG1 (hEAG, homolog of rEAG), with its corresponding YNL ligand motif: ligand interactions promote the occupation of early steps in the activation sequence, giving rise to the so-called Cole-Moore effect, and generally stabilize the open state of the channel (29). In zebrafish ELK, depolarizing prepulses potentiate current, but only when the intrinsic ligand is intact (26). An important unanswered question is how the conformation of the intrinsic ligand is communicated to the gating machinery. Its path to the channel gate via the C-linker seems most direct, yet a path to the VSD via the PAS-CNBh domain interaction can also be traced (30,31). Mutating the intrinsic ligand in hERG channels disrupts PAS-CNBh domain interactions, as demonstrated by FRET and gating assays, suggesting the intrinsic ligand is important for integrity of the intracellular ring in addition to its role in gating (28).

Given the observation that the intrinsic ligand promotes activation, it might reasonably be predicted that the open state of the KCNH channel is intrinsically liganded, and the closed state is not. Indeed, the concept of the “intrinsic ligand” inherently implies existence of an unliganded state. However, comparing the open hERG channel structure with the closed-gate rEAG1 structure, the ligand is clearly bound in both cases, suggesting it is not ejected from its binding site when the activation gate closes. Whether the ligand is bound in the true resting state of the channel, with the VSD in its “down” position and without CaM/Ca²⁺ bound, remains to be determined. Despite its invariance in the two

structures, in ELK channels, there is functional evidence that the intrinsic ligand is dynamic, rather than a fixed element of the channel’s tertiary structure: a peptide corresponding to the intrinsic ligand disrupts so-called voltage-dependent potentiation, as if competing for a binding pocket vacated by the intrinsic ligand. This result implies movement of the native intrinsic ligand and suggests its covalent linkage to other channel sequences is required to modulate channel function (32).

The “closed” conformation

What does comparison of the two proteins tell us about the channel gate? The structure of rEAG was determined with four molecules of CaM/Ca²⁺ bound to previously characterized cytosolic stretches immediately after the PAS domain (BDN) and CNBh domain (BDC1 and BDC2) (11,14). Intriguingly, each CaM protein interacts with three different subunits of the rEAG channel, including two on opposite sides of the channel (Fig. 3). Thus, binding of CaM is expected to stabilize or restrict movement in the PAS-CNBh ring, promoting a conformational state that favors closure of the gate despite having S4 in an upward position. It follows that quaternary arrangements of the PAS-CNBh rings should differ for hERG and rEAG, as observed for related CNG channels, in which superposition of two CNG channel structures in the open and closed states shows that binding of cyclic nucleotide results in a conformational change in the CNBh domain ring that is reflected in the splaying of S6 (33,34).

Surprisingly, comparison of the PAS-CNBh domain rings hERG and rEAG reveal only very subtle changes in the arrangement of the CNBh domains in the two rings

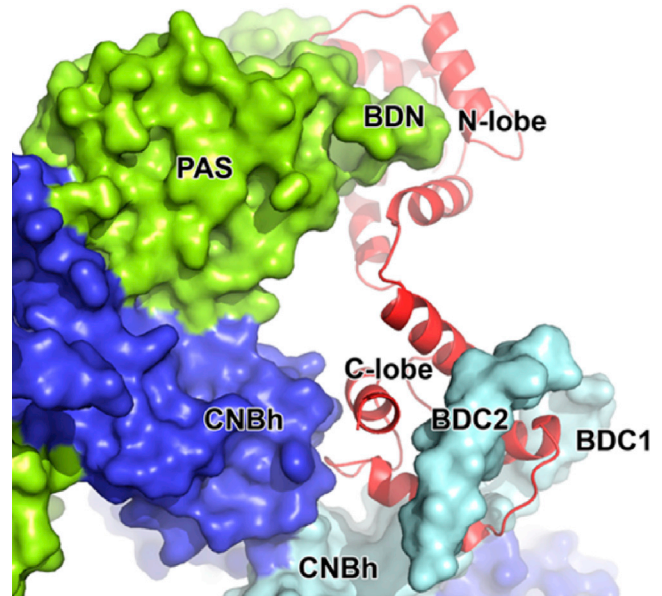


FIGURE 3 Calmodulin/Ca²⁺ bound to rEAG. A view from the cytosol of CaM/Ca²⁺ (red cartoon) associating with the cytosolic regions of three different subunits (cyan, blue, and light green surfaces) of the channel.

(Fig. 4). The root mean-square deviation for the α carbon ($C\alpha$) of residues in all four CNBh domains is ~ 0.9 Å, and the displacement of the $C\alpha$ from the aromatic residues in the intrinsic ligand of hERG (F from FNL) and rEAG (Y in YNL) is 0.5 Å. The largest differences occur between PAS domains, with the $C\alpha$ atom of equivalent residues in rEAG (P72) and hERG (E73) separated by 3.5 Å ($C\alpha$ atoms are indicated by spheres in Fig. 4). Instead, binding of CaM/Ca²⁺ and closure in rEAG result in a simple rigid-body rotation of the entire ring relative to hERG, paralleling the iris movement of $\alpha A'$ and $\alpha B'$ helices from the C-linker (Fig. 4). Therefore, the structural comparison of the open hERG and closed rEAG leaves unanswered the questions of how CaM/Ca²⁺ inhibits EAG channels and what the role of the PAS and CNBh domains in KCNH gating is. A possible explanation is that the closed-gate conformation mediated by CaM/Ca²⁺ is different from that elicited by voltage-dependent movements of the VSD. However, this argument is not supported by homology modeling of the hERG closed conformation, which mirrors details of the closed gate in the EAG cryo-EM structure (35).

Another obvious difference of the closed conformation can be appreciated in the pore cavity. In hERG channels, a “hydrophobic pocket” extends away from the pore cavity in the plane of the membrane just below the pore helices (Fig. 5; (1)). In the EAG1 structure, the hydrophobic pockets are squeezed shut (2). Whether these differences reflect open versus closed conformations or inherent differences between the channel types (see below) will require further study.

Mechanism of hERG block

At the time this manuscript was drafted, PubMed logged more than 3600 works with the search term “hERG or KCNH2,” making it the most examined member of the KCNH family.

Most of these studies focus on the curious and wanton property of hERG channels to avidly interact with a wide range of drugs and small molecules, presenting a major challenge for drug discovery and development (36). Because hERG channels conduct cardiac I_{Kr} (37,38), a repolarizing current in the heart (39), hERG blockers can prolong the ventricular action potential and the QT interval on the surface electrocardiogram and lead to catastrophic ventricular arrhythmias. Residues critical for drug block have been identified in the internal vestibule, where mutations (especially of F656 and Y652) alter efficacy of inhibition of many drugs by several orders of magnitude (40,41). Drug block requires an activated channel to allow drugs that have permeated the plasma membrane to exert their effects (42). Speculation that hERG’s pharmacophilia could arise from an unusually large central cavity was resoundingly quashed by new structural details showing that hERG’s vestibule is actually much smaller than those apparent in other open K channel structures (1). Electrostatic calculations suggest the pore helices entering hERG’s diminutive cavity yield a five-fold greater electronegativity compared with other K channels, providing a potentially powerful attraction to hERG blockers that are positively charged or can form cationic conjugate acids (1).

It has long been a curiosity that the closely related EAG1 channels do not exhibit the same high-affinity drug block, even though they possess the corresponding residues identified as critical for drug binding in the hERG cavity (43,44). Thus, comparing structures of the two channels is a sensible way to determine one of hERG’s most unique properties. The dimensions of the hydrophobic pocket off the pore cavity in the hERG structure will accommodate the aromatic moiety of a blocker, leading to speculation that the opportunity for binding does not exist in EAG1, where this pocket is constricted (1,2).

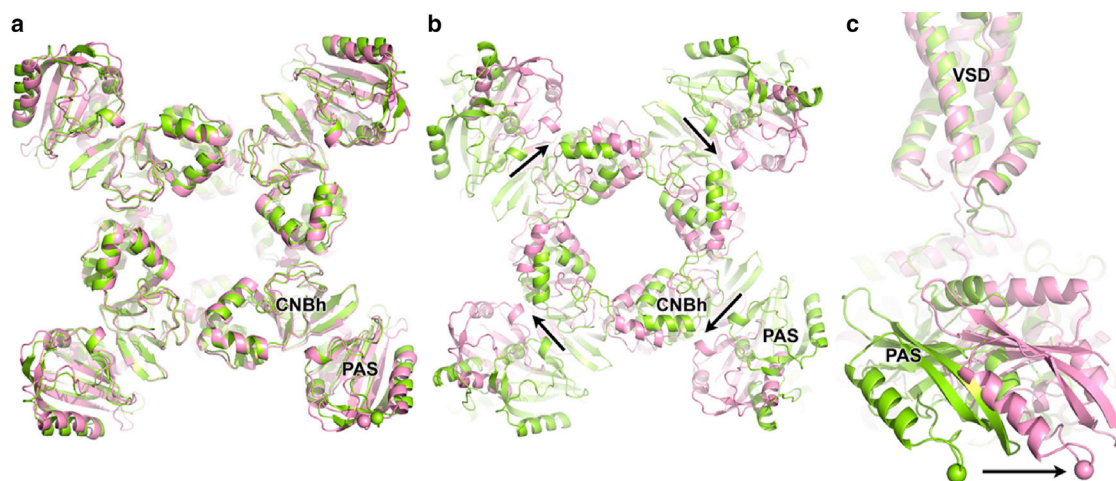


FIGURE 4 PAS-CNBh ring. Views from the cytosol of the PAS-CNBh domain rings: (a) structures after superposition of CNBh domains of rEAG (light green) and hERG (pink), (b) structures after superposition of the channels’ selectivity filters, and (c) side view of superposed channels through selectivity filter, showing PAS domains of rEAG (P72) and hERG (E73). Arrows indicated relative displacement. Spheres indicate in $C\alpha$ atom of equivalent residue in PAS domain of rEAG (P72) and hERG (E73).

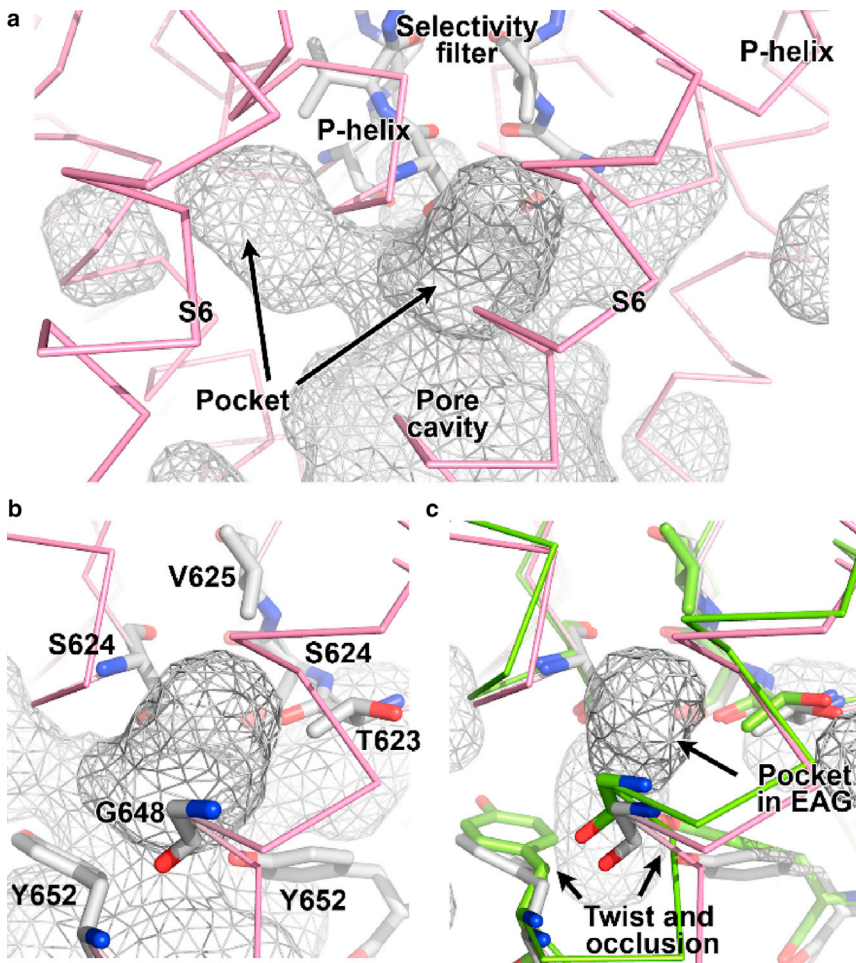


FIGURE 5 View of cavities in the pore of hERG. (a) View of the pore cavity shown as gray mesh with pockets jutting to the sides of the channel, just below the selectivity filter. Selectivity filter residues are shown as sticks. (b) Zoom view of one of the pockets with residues known to affect drug efficacy (Y652) lining the pocket shown as sticks and labeled. (c) Superposed rEAG (light green) and hERG (pink) channels viewed as in (b). The pocket in rEAG is shown as mesh, surrounded by the same residues as in (b) that are conserved in rEAG (shown as green stick). Slight twisting of tyrosine (Y652 in hERG) leads to isolation of the pocket from the pore cavity in rEAG.

The discovery of the hydrophobic pockets represents a paradigm shift in how KCNH channels, and particularly hERG, differ from other potassium channels. The pocket geometry may provide upper limits on how many drug molecules can bind, depending on the compound's dimensions. Close examination of the structures reveals that constriction of the hydrophobic pocket in rEAG is associated with a very small movement of the conserved tyrosine (Y652 in hERG; Fig. 5). Perhaps the hydrophobic pocket similarly constricts when the hERG channel closes, explaining the state dependence by which hERG blockers target only open (and/or inactivated) channels. And if the converse occurs, i.e., the EAG hydrophobic pockets become accessible in the open state, then the pockets cannot solely account for selective hERG block.

Inactivation

Of all things hERG, rapid inactivation is arguably the most iconic of the channel's properties. Inactivation occurs upon depolarization at a rate 10-fold that of activation, effectively suppressing outward current by severely limiting the

amount of time channels stay open upon depolarization (45,46). In this way, hERG inactivation allows sodium and calcium conductances to maintain ventricular depolarization for more than a whopping 300 ms (compared to <3 ms for a neuronal action potential). When membrane potential begins to flag, only then do hERG channels recover from inactivation and produce a resurgent current that decisively repolarizes the membrane (46). When inactivation is defective, repolarization happens too quickly, and catastrophic arrhythmias associated with short QT syndrome can result (47–50). EAG does not exhibit the powerful inactivation characteristic of hERG (24,51).

hERG inactivation occurs at the external mouth of the pore by a mechanism not well understood. It has the hallmarks of C-type inactivation, slowing with elevated K^+ concentrations or in the presence of external tetraethylammonium (TEA) (44,45,52,53). The N-terminus is involved but only as a modulator; N-terminal truncations slow the process (54), much like N-terminal truncations slow *Shaker* C-type inactivation (55). In other ion channels, inactivation borrows its voltage dependence from channel opening—when depolarization opens the channel, it subsequently

inactivates. In contrast, hERG inactivation is inherently voltage-dependent, as if directly gated by a voltage sensor (45,56). Cryo-EM structures are well-resolved at the selectivity filter and outer mouth of the pore for both the wild type and S631A, a mutant that impedes inactivation (57,58). Careful inspection reveals a slight shift of side chains at the outer reaches of the selectivity filter (1). It is a difference in the right location, where changes in angles of the side chains supporting ion flux is a plausible mechanism for inactivation. How the positions of these side chains are ultimately influenced by differences in transmembrane voltage cannot be gleaned considering all structures were determined at 0 mV.

A tantalizing link between inactivation and high-affinity drug block is based on reports that single point mutations disrupting one process also disrupt the other (44,52,59). “High-affinity” blockers such as dofetilide or E-4031 with IC_{50} values in the 1–10 nM range show loss of efficacy when inactivation is hampered by point mutations such as S620T or S631A flanking the pore selectivity sequence (44,52) or by other mutations in the vicinity (60). The connection between inactivation and block also occurs for some, but not all (60–62), lower-affinity blockers. Haloperidol, with an IC_{50} of 1 μ M, shows state dependence, an acceleration of inactivation in the presence of drug, and fourfold reduction of efficacy in the S631A mutation (58). Both inactivation and E-4031 sensitivity can be conferred upon mouse EAG by transferring a segment comprising much of the hERG selectivity filter and pore helix and the N-terminal half of the S6 transmembrane domain to the corresponding location in EAG. By effectively substituting only 15 residues, including outer mouth residues implicated in inactivation, EAG is transformed with the emblematic features of hERG (44). Ultimately, the link between inactivation and drug block could be elucidated by a structure clearly harboring a drug molecule, but the likelihood of structural resolution may be reduced by the occupancy of only one of four

possible binding sites in the pore cavity or hydrophobic pocket (1,63).

Slow deactivation in hERG

A distinctive functional feature of hERG is slow deactivation, which serves to delay channel closure upon repolarization long enough to allow the channels to recover from inactivation and provide a repolarizing surge of current at the appropriate time during the ventricular action potential (46). The impact of mutations and truncations of the N-terminus of the PAS domain (PAS-cap) on deactivation has been well described, with most speeding the process of channel closure (54,57,64,65). In addition, multiple functional studies have demonstrated interactions of the PAS-cap with residues in the C-linker and the S4-S5 linker (54,66–68). A comparison of hERG and rEAG structures offers a beautiful insight into the contribution of PAS-cap in gating (Fig. 6). In hERG, the two highly conserved N-terminal arginine residues of the PAS-cap are sequestered among one of the C-linker helices, the long S2-S3 loop characteristic of KCNH channels, and the region just upstream from the first transmembrane domain (pre-TM1). The structure also shows N-terminal residue V3 in contact distance of residues in the S4-S5 linker (Fig. 6 A). In rEAG, the closed gate is associated with repositioning of the C-linker away from the pre-TM1 region and S2-S3 loop, breaking apart the assembly that holds the PAS-cap in position. An accompanying disordering of part of the PAS-cap that includes the arginine residues is observed in the rEAG structure, in which L10 is the first residue seen in the structure. Thus, the structures indicate that when the gate is closed, the PAS-cap loosely interacts with the C-linker and VSD; in the open state, a binding site is assembled, and the PAS-cap becomes trapped. As a consequence, the PAS-cap stabilizes the gate in the open state by holding the C-linker in the open position. This model explains why mutations or truncations of the cap give rise to the very fast rate of deactivation in hERG.

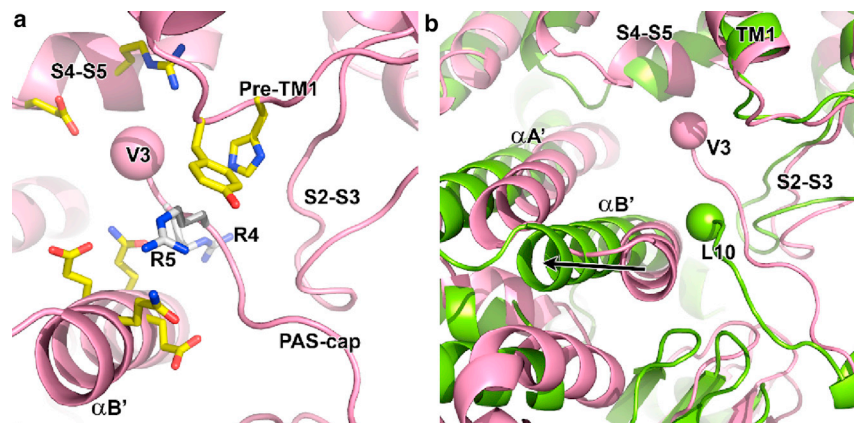


FIGURE 6 The PAS-cap binding site. (a) A zoom of the PAS-cap binding site in hERG; $C\alpha$ of V3 is shown as a sphere, and R4 and R5 are shown as white sticks. Residues within interacting distance (4 Å) of V3 and arginines are shown as yellow sticks. (b) A zoom of PAS-cap binding site in rEAG (light green) and hERG (pink) channels superposed through selectivity filter. Spheres indicate $C\alpha$ of first residue in PAS-cap: V3 (hERG) and L10 (rEAG). Arrow indicates movement of C-linker helix as the gate closes in rEAG, disassembling PAS-cap binding site.

Summary of unanswered questions

Cryo-EM and x-ray crystallography studies have provided unprecedented insights into the structural domains that so many of us have been tinkering with for so long. To say that not all questions have been answered is not to diminish this work's provocative contributions: the observation of the nonswapped architecture traded for swapped cytosolic domains, the idea of an intrinsic ligand, the subtle differences likely underlying inactivation, and the release of the PAS domain from a binding pocket accounting for slow deactivation. Still, there is much to keep us at it for some time to come. First, does the CNBh domain binding pocket become unliganded, and under what physiological conditions? What is the closed conformation of the resting hERG when the gate and VSD work in harmony? Will that resting conformation demonstrate a bigger difference in the PAS-CNBh ring between open and resting closed channel, in contrast to the small difference in EAG channel caught with its VSD up? How does the binding of CaM/Ca²⁺ lead to the closed EAG gate? How is drug binding in the hERG cavity and/or hydrophobic pocket transduced into block? Will new structures comparing a resting and inactivated hERG channel reveal how hERG inactivation gets its voltage dependence? More structures will no doubt help, together with the stalwart aid of targeted functional analysis.

ACKNOWLEDGMENTS

The authors thank Whitney Stevens-Sostre for comments.

This work was supported by National Institutes of Health grants 5R01NS081320-01A1 and 1R01HL131403-01A1 (G.A.R.) and by FEDER - Fundo Europeu de Desenvolvimento Regional funds through COMPETE 2020 - Operational Program for Competitiveness and Internationalization, Portugal 2020, and FCT - Fundação para a Ciência e a Tecnologia/Ministério da Ciência, Tecnologia e Ensino Superior in the framework of the project "Institute for Research and Innovation in Health Sciences" (POCI-01-0145-FEDER-007274) (J.H.M.-C.).

REFERENCES

1. Wang, W., and R. MacKinnon. 2017. Cryo-EM structure of the open human ether-a-go-go-related K(+) channel hERG. *Cell*. 169:422–430.e10.
2. Whicher, J. R., and R. MacKinnon. 2016. Structure of the voltage-gated K⁺ channel Eag1 reveals an alternative voltage sensing mechanism. *Science*. 353:664–669.
3. Lu, Z., A. M. Klem, and Y. Ramu. 2002. Coupling between voltage sensors and activation gate in voltage-gated K⁺ channels. *J. Gen. Physiol.* 120:663–676.
4. Lörinczi, É., J. C. Gómez-Posada, ..., L. A. Pardo. 2015. Voltage-dependent gating of KCNH potassium channels lacking a covalent link between voltage-sensing and pore domains. *Nat. Commun.* 6:6672.
5. de la Peña, P., P. Domínguez, and F. Barros. 2018. Functional characterization of Kv11.1 (hERG) potassium channels split in the voltage-sensing domain. *Pflugers Arch.* 470:1069–1085.
6. Lee, C. H., and R. MacKinnon. 2017. Structures of the human HCN1 hyperpolarization-activated channel. *Cell*. 168:111–120.e11.
7. James, Z. M., A. J. Borst, ..., D. Veessler. 2017. CryoEM structure of a prokaryotic cyclic nucleotide-gated ion channel. *Proc. Natl. Acad. Sci. USA*. 114:4430–4435.
8. Flynn, G. E., and W. N. Zagotta. 2018. Insights into the molecular mechanism for hyperpolarization-dependent activation of HCN channels. *Proc. Natl. Acad. Sci. USA*. 115:E8086–E8095.
9. Cowgill, J., V. A. Klenchin, ..., B. Chanda. 2019. Bipolar switching by HCN voltage sensor underlies hyperpolarization activation. *Proc. Natl. Acad. Sci. USA*. 116:670–678.
10. Schönherr, R., K. Löber, and S. H. Heinemann. 2000. Inhibition of human ether à go-go potassium channels by Ca(2+)/calmodulin. *EMBO J.* 19:3263–3271.
11. Ziechner, U., R. Schönherr, ..., S. H. Heinemann. 2006. Inhibition of human ether à go-go potassium channels by Ca²⁺/calmodulin binding to the cytosolic N- and C-termini. *FEBS J.* 273:1074–1086.
12. Gonçalves, J. T., and W. Stühmer. 2010. Calmodulin interaction with hEAG1 visualized by FRET microscopy. *PLoS One*. 5:e10873.
13. Lörinczi, E., M. Helliwell, ..., J. S. Mitcheson. 2016. Calmodulin regulates human ether à go-go 1 (hEAG1) potassium channels through interactions of the eag domain with the cyclic nucleotide binding homology domain. *J. Biol. Chem.* 291:17907–17918.
14. Marques-Carvalho, M. J., J. Oppermann, ..., J. H. Morais-Cabral. 2016. Molecular insights into the mechanism of calmodulin inhibition of the EAG1 potassium channel. *Structure*. 24:1742–1754.
15. Morais Cabral, J. H., A. Lee, ..., R. Mackinnon. 1998. Crystal structure and functional analysis of the HERG potassium channel N terminus: a eukaryotic PAS domain. *Cell*. 95:649–655.
16. Adaixo, R., C. A. Harley, ..., J. H. Morais-Cabral. 2013. Structural properties of PAS domains from the KCNH potassium channels. *PLoS One*. 8:e59265.
17. Guy, H. R., S. R. Durell, ..., B. Ganetzky. 1991. Similarities in amino acid sequences of Drosophila eag and cyclic nucleotide-gated channels. *Science*. 254:730.
18. Brelidze, T. I., A. E. Carlson, ..., W. N. Zagotta. 2012. Structure of the carboxy-terminal region of a KCNH channel. *Nature*. 481:530–533.
19. Haitin, Y., A. E. Carlson, and W. N. Zagotta. 2013. The structural mechanism of KCNH-channel regulation by the eag domain. *Nature*. 501:444–448.
20. Henry, J. T., and S. Crosson. 2011. Ligand-binding PAS domains in a genomic, cellular, and structural context. *Annu. Rev. Microbiol.* 65:261–286.
21. McIntosh, B. E., J. B. Hogenesch, and C. A. Bradfield. 2010. Mammalian Per-Arnt-Sim proteins in environmental adaptation. *Annu. Rev. Physiol.* 72:625–645.
22. Möglich, A., R. A. Ayers, and K. Moffat. 2009. Structure and signaling mechanism of Per-ARNT-Sim domains. *Structure*. 17:1282–1294.
23. Brelidze, T. I., A. E. Carlson, and W. N. Zagotta. 2009. Absence of direct cyclic nucleotide modulation of mEAG1 and hERG1 channels revealed with fluorescence and electrophysiological methods. *J. Biol. Chem.* 284:27989–27997.
24. Robertson, G. A., J. M. Warmke, and B. Ganetzky. 1996. Potassium currents expressed from Drosophila and mouse eag cDNAs in Xenopus oocytes. *Neuropharmacology*. 35:841–850.
25. Marques-Carvalho, M. J., N. Sahoo, ..., J. H. Morais-Cabral. 2012. Structural, biochemical, and functional characterization of the cyclic nucleotide binding homology domain from the mouse EAG1 potassium channel. *J. Mol. Biol.* 423:34–46.
26. Dai, G., and W. N. Zagotta. 2017. Molecular mechanism of voltage-dependent potentiation of KCNH potassium channels. *eLife*. 6:e26355.
27. Harley, C. A., G. Starek, ..., J. H. Morais-Cabral. 2016. Enhancement of hERG channel activity by scFv antibody fragments targeted to the PAS domain. *Proc. Natl. Acad. Sci. USA*. 113:9916–9921.
28. Coddling, S. J., and M. C. Trudeau. 2019. The hERG potassium channel intrinsic ligand regulates N- and C-terminal interactions and channel closure. *J. Gen. Physiol.* 151:478–488.

29. Zhao, Y., M. P. Goldschen-Ohm, ..., G. A. Robertson. 2017. The intrinsically liganded cyclic nucleotide-binding homology domain promotes KCNH channel activation. *J. Gen. Physiol.* 149:249–260.
30. de la Peña, P., C. Alonso-Ron, ..., F. Barros. 2011. Demonstration of physical proximity between the N terminus and the S4-S5 linker of the human ether-a-go-go-related gene (hERG) potassium channel. *J. Biol. Chem.* 286:19065–19075.
31. Tan, P. S., M. D. Perry, ..., A. P. Hill. 2012. Voltage-sensing domain mode shift is coupled to the activation gate by the N-terminal tail of hERG channels. *J. Gen. Physiol.* 140:293–306.
32. Dai, G., Z. M. James, and W. N. Zagotta. 2018. Dynamic rearrangement of the intrinsic ligand regulates KCNH potassium channels. *J. Gen. Physiol.* 150:625–635.
33. Li, M., X. Zhou, ..., J. Yang. 2017. Structure of a eukaryotic cyclic nucleotide-gated channel. *Nature.* 542:60–65.
34. Rheinberger, J., X. Gao, ..., C. M. Nimigean. 2018. Ligand discrimination and gating in cyclic nucleotide-gated ion channels from apo and partial agonist-bound cryo-EM structures. *eLife.* 7:e39775.
35. Wynia-Smith, S. L., A. L. Gillian-Daniel, ..., G. A. Robertson. 2008. hERG gating microdomains defined by S6 mutagenesis and molecular modeling. *J. Gen. Physiol.* 132:507–520.
36. Windley, M. J., N. Abi-Gerges, ..., A. P. Hill. 2017. Measuring kinetics and potency of hERG block for CiPA. *J. Pharmacol. Toxicol. Methods.* 87:99–107.
37. Sanguinetti, M. C., C. Jiang, ..., M. T. Keating. 1995. A mechanistic link between an inherited and an acquired cardiac arrhythmia: HERG encodes the IKr potassium channel. *Cell.* 81:299–307.
38. Trudeau, M. C., J. W. Warmke, ..., G. A. Robertson. 1995. HERG, a human inward rectifier in the voltage-gated potassium channel family. *Science.* 269:92–95.
39. Sanguinetti, M. C., and N. K. Jurkiewicz. 1990. Two components of cardiac delayed rectifier K⁺ current. Differential sensitivity to block by class III antiarrhythmic agents. *J. Gen. Physiol.* 96:195–215.
40. Mitcheson, J., M. Perry, ..., J. Hancox. 2005. Structural determinants for high-affinity block of hERG potassium channels. *Novartis Found. Symp.* 266:136–150, discussion 150–158.
41. Mitcheson, J. S., J. Chen, ..., M. C. Sanguinetti. 2000. A structural basis for drug-induced long QT syndrome. *Proc. Natl. Acad. Sci. USA.* 97:12329–12333.
42. Snyders, D. J., and A. Chaudhary. 1996. High affinity open channel block by dofetilide of HERG expressed in a human cell line. *Mol. Pharmacol.* 49:949–955.
43. Ficker, E., W. Jarolimek, ..., A. M. Brown. 1998. Molecular determinants of dofetilide block of HERG K⁺ channels. *Circ. Res.* 82:386–395.
44. Herzberg, I. M., M. C. Trudeau, and G. A. Robertson. 1998. Transfer of rapid inactivation and sensitivity to the class III antiarrhythmic drug E-4031 from HERG to M-eag channels. *J. Physiol.* 511:3–14.
45. Spector, P. S., M. E. Curran, ..., M. C. Sanguinetti. 1996. Fast inactivation causes rectification of the IKr channel. *J. Gen. Physiol.* 107:611–619.
46. Zhou, Z., Q. Gong, ..., C. T. January. 1998. Properties of HERG channels stably expressed in HEK 293 cells studied at physiological temperature. *Biophys. J.* 74:230–241.
47. Brugada, R., K. Hong, ..., C. Antzelevitch. 2004. Sudden death associated with short-QT syndrome linked to mutations in HERG. *Circulation.* 109:30–35.
48. McPate, M. J., R. S. Duncan, ..., J. C. Hancox. 2005. The N588K-HERG K⁺ channel mutation in the ‘short QT syndrome’: mechanism of gain-in-function determined at 37 degrees C. *Biochem. Biophys. Res. Commun.* 334:441–449.
49. McPate, M. J., H. J. Witchel, and J. C. Hancox. 2006. Short QT syndrome. *Future Cardiol.* 2:293–301.
50. McPate, M. J., H. Zhang, ..., J. C. Hancox. 2009. Comparative effects of the short QT N588K mutation at 37 degrees C on hERG K⁺ channel current during ventricular, Purkinje fibre and atrial action potentials: an action potential clamp study. *J. Physiol. Pharmacol.* 60:23–41.
51. Ludwig, J., H. Terlau, ..., O. Pongs. 1994. Functional expression of a rat homologue of the voltage gated ether a go-go potassium channel reveals differences in selectivity and activation kinetics between the Drosophila channel and its mammalian counterpart. *EMBO J.* 13:4451–4458.
52. Ficker, E., W. Jarolimek, and A. M. Brown. 2001. Molecular determinants of inactivation and dofetilide block in ether a-go-go (EAG) channels and EAG-related K(+) channels. *Mol. Pharmacol.* 60:1343–1348.
53. Smith, P. L., T. Baukowitz, and G. Yellen. 1996. The inward rectification mechanism of the HERG cardiac potassium channel. *Nature.* 379:833–836.
54. Wang, J., M. C. Trudeau, ..., G. A. Robertson. 1998. Regulation of deactivation by an amino terminal domain in human ether-a-go-go-related gene potassium channels. *J. Gen. Physiol.* 112:637–647.
55. Hoshi, T., W. N. Zagotta, and R. W. Aldrich. 1990. Biophysical and molecular mechanisms of Shaker potassium channel inactivation. *Science.* 250:533–538.
56. Wang, S., M. J. Morales, ..., R. L. Rasmusson. 1996. Time, voltage and ionic concentration dependence of rectification of h-erg expressed in Xenopus oocytes. *FEBS Lett.* 389:167–173.
57. Schönherr, R., and S. H. Heinemann. 1996. Molecular determinants for activation and inactivation of HERG, a human inward rectifier potassium channel. *J. Physiol.* 493:635–642.
58. Suessbrich, H., R. Schönherr, ..., A. E. Busch. 1997. The inhibitory effect of the antipsychotic drug haloperidol on HERG potassium channels expressed in Xenopus oocytes. *Br. J. Pharmacol.* 120:968–974.
59. Lees-Miller, J. P., Y. Duan, ..., H. J. Duff. 2000. Molecular determinant of high-affinity dofetilide binding to HERG1 expressed in Xenopus oocytes: involvement of S6 sites. *Mol. Pharmacol.* 57:367–374.
60. Perrin, M. J., P. W. Kuchel, ..., J. I. Vandenberg. 2008. Drug binding to the inactivated state is necessary but not sufficient for high-affinity binding to human ether-a-go-go-related gene channels. *Mol. Pharmacol.* 74:1443–1452.
61. Sánchez-Chapula, J. A., R. A. Navarro-Polanco, ..., M. C. Sanguinetti. 2002. Molecular determinants of voltage-dependent human ether-a-go-go related gene (HERG) K⁺ channel block. *J. Biol. Chem.* 277:23587–23595.
62. Kamiya, K., J. S. Mitcheson, ..., M. C. Sanguinetti. 2001. Open channel block of HERG K(+) channels by vesnarinone. *Mol. Pharmacol.* 60:244–253.
63. Vandenberg, J. I., E. Perozo, and T. W. Allen. 2017. Towards a structural view of drug binding to hERG K⁺ channels. *Trends Pharmacol. Sci.* 38:899–907.
64. Chen, J., A. Zou, ..., M. C. Sanguinetti. 1999. Long QT syndrome-associated mutations in the Per-Arnt-Sim (PAS) domain of HERG potassium channels accelerate channel deactivation. *J. Biol. Chem.* 274:10113–10118.
65. Wang, J., C. D. Myers, and G. A. Robertson. 2000. Dynamic control of deactivation gating by a soluble amino-terminal domain in HERG K(+) channels. *J. Gen. Physiol.* 115:749–758.
66. Ng, C. A., K. Phan, ..., M. D. Perry. 2014. Multiple interactions between cytoplasmic domains regulate slow deactivation of Kv11.1 channels. *J. Biol. Chem.* 289:25822–25832.
67. Fernández-Trillo, J., F. Barros, ..., P. de la Peña. 2011. Molecular determinants of interactions between the N-terminal domain and the transmembrane core that modulate hERG K⁺ channel gating. *PLoS One.* 6:e24674.
68. Hull, C. M., S. Sokolov, ..., T. W. Claydon. 2014. Regional flexibility in the S4-S5 linker regulates hERG channel closed-state stabilization. *Pflugers Arch.* 466:1911–1919.